



Stagnation flow thermophoretic deposition with variable particle concentration in the mainstream

Frank K. Hsu, Ralph Greif *

Department of Mechanical Engineering, University of California at Berkeley, Berkeley, CA 94720-1740, USA

Received 27 December 2000; received in revised form 30 June 2001

Abstract

A methodology for determining deposition with thermophoretic transport is introduced. An application is made to stagnation flow. The classical similarity solution for stagnation flow requires the boundary condition of a uniform particle concentration at an infinite location away from the wall. The present methodology removes these restrictions; i.e., it is valid for a spatially variable particle concentration boundary condition at a finite distance from the wall. The deposition characteristics are presented in terms of a factor F . The dependence of F on the flow parameters is studied and discussed. © 2002 Published by Elsevier Science Ltd.

1. Introduction

There are many systems that require the attainment of high particle deposition efficiency and the precise control of the deposition to minimize costs and maximize the quality of the finished product. High efficiency and control of deposition determine the success of chemical vapor deposition systems. Understanding stagnation deposition is important because several deposition processes consist of flows that are impinging on solid surfaces [1].

Gokoglu and Rosner [2,3], Stratmann et al. [4], Garg and Jayaraj [5,6], and Kusanadi and Greif [7] carried out studies of stagnation flow with thermophoretic transport. The thermophoretic force [8] causes submicron sized particles to move from hot to cold regions. Gokoglu and Rosner [2,3] carried out comprehensive studies of the mass transfer in boundary layer flows and included variable properties and covered a broad range of conditions. Stratmann et al. [4] considered a hot wall so that the thermophoretic force repels the particles and a particle free zone can form near the hot surface. Garg and Jayaraj [5,6] studied particle deposition on a cylinder. Kusanadi and

Greif [7] included the effects of electrophoretic and thermophoretic forces on stagnation deposition. In all of the above works, the inlet boundary condition is for a uniform particle distribution.

In the present work, the inlet particle distribution is non-uniform. Specific results are obtained for a constant particle distribution, C_1 , over a central region and a zero concentration outside this region, but the methodology developed in this work is valid for a general non-uniform particle distribution. A non-uniform condition more closely resembles the actual process which contains particle generation in the central portion of a burner. Indeed, Graham and Alam [9] utilized the FLUENT code to determine the thermophoretic transport for a non-uniform inlet condition in their study of the outside vapor deposition process.

2. Configuration and conditions

The study is that of stagnation flow with particle deposition due to thermophoresis. A schematic diagram of the system is illustrated in Fig. 1. The x -direction is parallel to the deposition surface and the y -direction is perpendicular to the surface. The origin of the coordinate system, $x = 0$, $y = 0$, is at the stagnation point. The flow at a temperature of T_∞ is moving towards the wall which is at a constant temperature of T_w . At a location

* Corresponding author. Tel.: +1-510-642-6462; fax: +1-510-642-5539.

E-mail address: greif@newton.me.berkeley.edu (R. Greif).

Nomenclature		Greek Letter	
b	non-dimensional wall temperature; $b = \frac{T_w}{T_\infty - T_w}$	δ	boundary layer thickness
C	mass concentration	Φ	deposition efficiency
F	factor	η	non-dimensional distance
J	deposition flux	ν	kinematic viscosity
K	thermophoretic coefficient	θ	non-dimensional temperature; $\theta = \frac{T - T_w}{T_\infty - T_w}$
Kn	Knudsen number; $Kn \equiv \lambda/d_p$	ψ	stream function
Pr	Prandtl number; $Pr \equiv \nu/\alpha$	\wp	mass diffusivity
Sc	Schmidt number; $Sc \equiv \nu/\wp$	<i>Subscript</i>	
T	temperature	FZ	particle free zone
u	velocity in x direction	i	inlet
U	inlet velocity in x direction	I	inlet location
v	velocity in y direction	p	particle
V	inlet velocity in y direction	th	thermophoretic
x	direction parallel to the wall	TH	thermal boundary layer
y	direction perpendicular to the wall	velocity	velocity boundary layer
		w	wall
		δ	boundary layer thickness
		∞	infinite

$y = y_1$, the incoming flow has a specified non-uniform particle distribution according to the following conditions:

$$|x| \leq |x_1|, C(x, y_1) = C_1; \quad |x| > |x_1|, C(x, y_1) = 0. \quad (1)$$

The concentration of the particles is assumed to be small and the flow field is not disturbed by the presence of the particles. The size of the particles is assumed to be small and the particles follow the gas flow in the isothermal region. The flow properties are assumed to be constant. The particle Schmidt number, $Sc = \nu/\wp_p$, is assumed to be large (the particle diffusivity \wp_p is small) and particle diffusion due to the particle concentration difference is neglected. Thermophoresis is the only effect considered

that causes the particle trajectory to deviate from the gas streamline.

3. Analysis

The analysis begins with the presentation of the velocity and the temperature similarity solutions, which is followed by the particle distribution and deposition analysis.

3.1. Gas velocities and temperature

The governing equations and boundary conditions for two-dimensional stagnation boundary layer flow are given by Goldstein [10], White [11], Stratmann et al. [4], Schlichting [12], and are not repeated here. The velocity distribution for stagnation flow in the frictionless potential flow region is given by:

$$U = ax; \quad V = -ay. \quad (2)$$

In the viscous flow region, the velocity distribution is assumed to have the following form:

$$u = xg'(y); \quad v = -g(y), \quad (3)$$

and the stream function is given by:

$$\psi = xg(y). \quad (4)$$

Introducing the dimensionless variables,

$$\eta = \sqrt{\frac{a}{\nu}}y, \quad \text{and} \quad g(y) = \sqrt{a\nu}f(\eta), \quad (5)$$

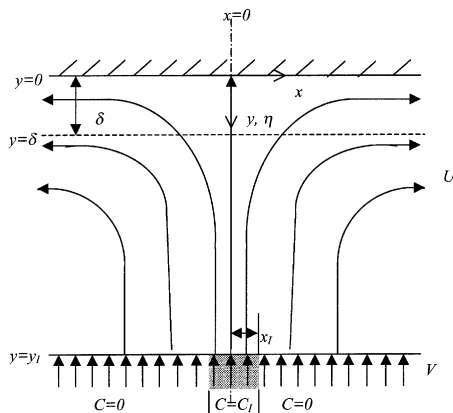


Fig. 1. Schematic diagram of stagnation flow gas streamlines.

the velocity distribution is rewritten in the following form:

$$u = axf'(\eta); \quad v = -\sqrt{av}f(\eta). \quad (6)$$

Utilizing Eqs. (5) and (6), the momentum equation and the boundary conditions are transformed into the following dimensionless equations [12]:

$$f''' + ff'' - f'^2 + 1 = 0, \quad (7)$$

$$f = 0, \quad f' = 0 \text{ at } \eta = 0; \quad f' = 1, \quad \eta \rightarrow \infty, \quad (8)$$

and tabulated solutions can be found in Schlichting [12].

Introducing

$$\theta = \frac{T - T_w}{T_\infty - T_w}, \quad (9)$$

the energy equation and the boundary conditions become:

$$\theta'' + Prf\theta' = 0, \quad (10a)$$

and

$$\theta = 0, \text{ at } \eta = 0; \quad \theta = 1, \quad \eta \rightarrow \infty. \quad (10b)$$

The energy equation has the closed form solution [10]:

$$\theta(\eta) = \frac{\int_0^\eta \exp(-Pr \int_0^\xi f(\zeta) d\zeta) d\xi}{\int_0^\infty \exp(-Pr \int_0^\xi f(\zeta) d\zeta) d\xi}. \quad (11)$$

3.2. Particle deposition

In previous particle deposition studies, the inlet particle distribution is required to be uniform. In the current study, the distribution is non-uniform with particles at the inlet only present in a region $\pm x_i$ around the centerline as indicated in Fig. 1. A streamline/particle pathline approach is used to determine the particle trajectories and the relationship between the particle inlet and deposition locations.

The flow field is assumed to be unaltered by the particles. The region outside the thermal boundary layer is isothermal and in this outer region, particles do not experience the thermophoretic force which causes the particles to deviate from the gas streamline. The particle trajectory analysis is divided into two regions; one outside the thermal boundary layer (no thermophoretic force) and one inside the thermal boundary layer (with the thermophoretic force).

The particle paths in the isothermal region outside the thermal boundary layer are identical to the gas phase streamlines. Using the streamline definition, $\frac{dy}{dx}|_{\text{streamline}} = \frac{v}{u}$ yields:

$$\frac{dy}{dx}|_{\text{streamline}} = \frac{-g(y)}{xg'(y)}, \text{ or } \frac{d\eta}{dx}|_{\text{streamline}} = \frac{-f(\eta)}{xf'(\eta)}. \quad (12)$$

The velocity boundary layer thickness is obtained from $f'(\eta_{\delta, \text{velocity}}) = 0.99$, which yields $\eta_{\delta, \text{velocity}} = 2.4$.

Within the thermal boundary layer, the thermophoretic force is present. The similarity result gives that the temperature and the thermophoretic force only vary in the y or η direction (Eq. (11)). The thermophoretic velocity is written as [13]

$$v_{\text{th}} = -\frac{Kv}{T} \frac{dT}{dy} = \frac{-\sqrt{av}K\theta'}{\theta + b}, \quad b = \frac{T_w}{T_\infty - T_w}. \quad (13)$$

The particle velocity is the sum of the gas and the thermophoretic velocities; $v_p = v + v_{\text{th}}$. Combining the gas velocity, Eq. (6), and the thermophoretic velocity, Eq. (13), the relation for the particle path inside the thermal boundary layer becomes:

$$\frac{dy}{dx} = \frac{-\sqrt{av}\left(f(\eta) + \frac{K\theta'(\eta)}{\theta(\eta)+b}\right)}{axf'(\eta)} \text{ or } \frac{d\eta}{dx} = \frac{-\left(f(\eta) + \frac{K\theta'(\eta)}{\theta(\eta)+b}\right)}{xf'(\eta)}, \quad (14)$$

which can be solved by separating the variables. The result relating the particle deposition location on the wall ($x_w, 0$) to the particle location at the thermal boundary layer ($x_{\delta_{\text{TH}}}, \eta_{\delta_{\text{TH}}}$), is:

$$\frac{x_w}{x_{\delta_{\text{TH}}}} = \exp\left(\int_0^{\eta_{\delta_{\text{TH}}}} \frac{f'}{f + \frac{K\theta'}{\theta+b}} d\eta\right). \quad (15)$$

The thermophoretic force causes the particles to deviate from the gas streamlines inside the thermal boundary layer.

The relationship between the particle deposition location on the solid wall x_w and the particle location (x_i, y_i) outside the thermal boundary layer can be obtained by matching the particle paths inside and outside the thermal boundary layer at the thermal boundary layer. Outside the thermal boundary layer, the particles follow the gas streamlines. Therefore, the particle trajectory between a location outside the thermal boundary layer (x_i, y_i) and its location at the thermal boundary layer ($x_{\delta_{\text{TH}}}, y_{\delta_{\text{TH}}}$) can be determined from

$$\begin{aligned} \psi(x_i, y_i) &= x_i g(y_i) = \psi(x_{\delta_{\text{TH}}}, y_{\delta_{\text{TH}}}) = x_{\delta_{\text{TH}}} g(y_{\delta_{\text{TH}}}) \\ \Rightarrow x_{\delta_{\text{TH}}} &= x_i \frac{g(y_i)}{g(y_{\delta_{\text{TH}}})} = x_i \frac{f(\eta_i)}{f(\eta_{\delta_{\text{TH}}})}. \end{aligned} \quad (16)$$

Combining Eqs. (15) and (16), the relationship between the particle deposition location on the wall and the particle location outside the thermal boundary layer is

$$\begin{aligned} F \equiv \frac{x_w}{x_i} &= \frac{g(y_i)}{g(y_{\delta_{\text{TH}}})} \exp\left(\int_0^{\eta_{\delta_{\text{TH}}}} \frac{f'}{f + \frac{K\theta'}{\theta+b}} d\eta\right) \\ &= \frac{f(\eta_i)}{f(\eta_{\delta_{\text{TH}}})} \exp\left(\int_0^{\eta_{\delta_{\text{TH}}}} \frac{f'}{f + \frac{K\theta'}{\theta+b}} d\eta\right). \end{aligned} \quad (17)$$

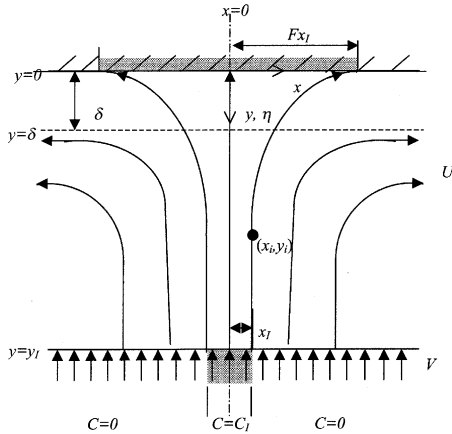


Fig. 2. Schematic diagram of stagnation deposition – particle pathlines.

For a constant particle concentration within $|x| \leq |x_1|$ at the inlet elevation y_1 , and no particles present for $|x| > |x_1|$ at y_1 , all of the particle deposition on the wall takes place within $\pm F|x_1|$ of the stagnation point (cf. Eq. (17), with $F > 1$), as shown in Fig. 2. Note that if the thermophoretic coefficient, K , equals zero, integrating the right-hand side of Eq. (17) yields $\ln(f(\eta_\delta)) - \ln(f(0))$ and F approaches infinity. This corresponds to no deposition of particles; note that for K equals zero, the particles follow the gas streamlines and there is no deposition. At the other extreme, K approaching infinity, the thermophoretic velocity approaches infinity. For this condition, the exponential term in Eq. (17) equals unity (the integrand and therefore the integral equal zero). Eq. (17) then becomes $F = x_w/x_i = g(y_1)/g(y_{\delta TH}) = f(\eta_i)/f(\eta_{\delta TH})$. Utilizing Eq. (16), this yields $x_w = x_\delta$, which corresponds to a “sudden” deposition once the particles reach the thermal boundary layer.

The particle inlet flux is given by $J_1(x_i) = C_1(x_i)V_{P,1} = C_1(x_i)V_1$ (where $V_{th,1} = 0$ and $V_{P,1} = V_{gas,1} = V_1$). Note that the inlet flux (at $y_1 = y_1, |x_i| \leq |x_1|$), $J_1 = C_1V_1$, is constant for constant C_1 because $V_1 = -ay_1$. The deposition flux on the wall can be determined by considering two particle paths starting at inlet locations (x_i, y_1) and at $(x_i + \varepsilon_i, y_1)$. The corresponding deposition locations on the wall, $y = 0$, are $(F(x_i), 0)$ and $(F(x_i + \varepsilon_i), 0)$, respectively. The length between the two streamlines at the inlet elevation y_1 is ε_i and on the wall the length is $F\varepsilon_i$, which is F times larger than the length at the inlet elevation. The total particle flow rate between these two streamlines is constant at every elevation y . The local deposition flux on the wall at $x_w = Fx_i, J_w(x_w)$, is obtained from

$$J_1(x_i)\varepsilon_i = J_w(x_w)\varepsilon_w = J_w(Fx_i)F\varepsilon_i \Rightarrow J_w(Fx_i) = \frac{J_1(x_i)}{F} \tag{18}$$

For the boundary condition with a constant injection particle concentration within $\pm|x_1|$ at the inlet elevation y_1 and a deposition region within $\pm|x_w| (|x_w| = F|x_1|)$, Eq. (18) becomes

$$J_w = \frac{J_1}{F} \tag{19}$$

The total deposition (from $-x_w$ to x_w) for a uniform inlet particle concentration from $-x_1$ to x_1 is $\int_{-x_1}^{x_1} J_1 dx = J_1 2x_1 = \int_{-x_w}^{x_w} J_w dx = J_w 2x_w$. The local deposition flux is uniform from $-x_w$ to x_w .

The deposition efficiency i.e., the fraction of the total particles injected that is deposited within a region from x_A to x_B is given as

$$\Phi = \frac{\int_{x_A}^{x_B} C_w(x)V_{P,w}(x) dx}{V_P(y_1) \int_{-x_1}^{x_1} C_1(x) dx} = \frac{\int_{x_A}^{x_B} J_w(x) dx}{\int_{-x_1}^{x_1} J_1(x) dx} = \frac{\int_{x_A}^{x_B} J_1(x_i) dx_i}{\int_{-x_1}^{x_1} J_1(x) dx} = \frac{\int_{x_{A/F}}^{x_{B/F}} J_1(x_j) dx_j}{\int_{-x_1}^{x_1} J_1(x) dx} \tag{20}$$

where $V_{P,w} = V_{th,w}$ because the gas velocity at the wall is zero.

Over a deposition region of $\pm|x|$ (where $|x| < F|x_1|$) and with a boundary condition of a constant inlet particle concentration within $\pm|x_1|$ at the inlet elevation y_1 , Eq. (20) becomes

$$\Phi = \frac{(J_1/F)2x}{J_1 2x_1} = \frac{x}{x_1 F} \tag{21}$$

To increase the deposition over a length $\pm|x|$ requires that the particles collected within this region be increased. One way to achieve this goal is to minimize the value of F ; see Eqs. (20) and (21). The factor F depends on the flow field conditions; e.g., the temperatures of the wall and the inlet gas, the Prandtl number of the gas, and the thermophoretic constant K , which is a function of particle size. The effects of these parameters on deposition are considered below. Another consideration is the particle concentration distribution at the inlet elevation. High concentrations with small values of $|x_1|$ at the inlet elevation, y_1 , will yield a large particle deposition near the stagnation point.

It is pointed out that Eqs. (18) and (20) are also valid for more general particle concentration inlet conditions including, for example, a spatially variable particle concentration within $\pm|x_1|$ at the inlet elevation y_1 and zero concentration outside this region. Also note that the particle concentration distribution and the region of deposition efficiency (Eq. (20)) need not be symmetric at the inlet.

3.3. Particle free zone

For a cold wall, the thermophoretic force from a hot gas towards the cold wall results in deposition. Strat-

mann et al. [4] studied a hot wall so that the thermophoretic force is away from the wall and a particle free zone results with no deposition. The particle free zone thickness can be determined by determining the elevation at which the component of velocity perpendicular to the wall equals zero or by locating the elevation where the particle streamline has a zero slope; i.e., $d\eta/dx = 0$. Equating Eq. (14) to zero, the particle free zone thickness can be determined from the following relation:

$$f + \frac{K\theta'}{\theta + b} = 0. \tag{22}$$

Near the wall, Stratmann et al. [4] use:

$$f = 0.5\beta\eta^2, \tag{23a}$$

$$\beta = \left. \frac{d^2f}{d\eta^2} \right|_{\eta=0} = 1.2326 \text{ (plane stagnation flow)} \tag{23b}$$

$$\theta = 0 \text{ and } \theta' = 0.5692Pr^{0.377}, \text{ as } \eta \rightarrow 0. \tag{23c, d}$$

Substituting Eqs. (23a)–(d) into Eq. (22) yields the same results as Stratmann et al. [4] for the particle free zone thickness, namely,

$$\eta_{FZ} = 0.961K^{0.5} \left(\frac{T_w - T_\infty}{T_w} \right)^{0.5} Pr^{0.189}, \tag{24}$$

or

$$\delta_{FZ} = 0.961K^{0.5} \left(\frac{v}{a} \right)^{0.5} \left(\frac{T_w - T_\infty}{T_w} \right)^{0.5} Pr^{0.189}. \tag{25}$$

4. Discussion

An important characteristic of stagnation deposition is the factor, F . The deposition length, $x_w = Fx_i$, is obtained once F is obtained. A small value of $F = x_w/x_i$ means the particles travel a smaller distance parallel to the wall before depositing. Thus the deposition length is smaller and the deposition flux is larger for a small value of F . In this section, the dependence of F on the system parameters is investigated. Important parameters include: b , defined in terms of the inlet flow temperature and wall temperature, η_i , the particle inlet elevation, K , the thermophoretic coefficient, and Pr , the Prandtl number. The inlet particle concentration is specified at the plane, $\eta = \eta_i$, according to Eq. (1).

The numerical solution of Eq. (17) is obtained by using MathCAD® Version 8. To resolve the boundary layer, a total of 60 uniformly spaced points are used over the range from $\eta = 0$ to 6. Calculations were also made for a total of 120 uniformly spaced points from $\eta = 0$ to

6 for the conditions of $b = 0.1$ and 1.0, with $\eta_i = 10.0$, $K = 0.55$, and $Pr = 0.7$. The comparison of the values of F using these two sets of grid numbers yields differences of 0.7% ($b = 1.0$) and 2.9% ($b = 0.1$). A total of 60 grid points over the range from $\eta = 0$ to 6 is sufficient for the present analysis. The thermal boundary layer thickness is defined as the elevation when the local non-dimensional temperature reaches 0.99, $\theta = 0.99$. The thermal boundary thickness is a function of Pr . For $Pr = 0.7$, the thermal boundary layer thickness is $\eta_{TH} = 3.5$ (also refer to Stratmann et al. [4]).

The base line conditions are:

$$b = 0.5, \quad \eta_i = 10.0, \quad K = 0.55, \text{ and } Pr = 0.7. \tag{26}$$

4.1. Dependence on thermophoretic coefficient, K

The factor $F = x_w/x_i$ is calculated over a range of values of the thermophoretic coefficient, K , from 0.1 to 10 with the other parameters at the baseline values of Eq. (26). The value of F decreases for increasing K as shown in Fig. 3. A larger value of K results in a larger thermophoretic force and thus a shorter distance parallel to the wall is traveled before deposition; i.e., $F = x_w/x_i$ decreases. The deposition flux increases with increasing K . K is large (F is small) when Kn is large [13]. Kn is large when the particles are small or if the pressure is low; i.e., the mean free path is large; thus, the factor F is small and the deposition flux is large when the particles are small.

4.2. Dependence on $b = T_w/(T_\infty - T_w)$

The factor $F = x_w/x_i$ is calculated over a range of values of the non-dimensional wall temperature b

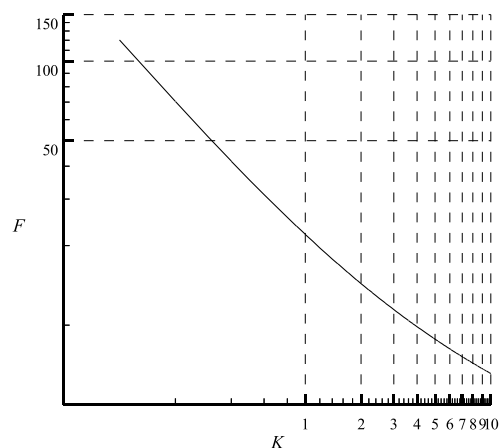


Fig. 3. The variation of the factor F with respect to the thermophoretic coefficient K .

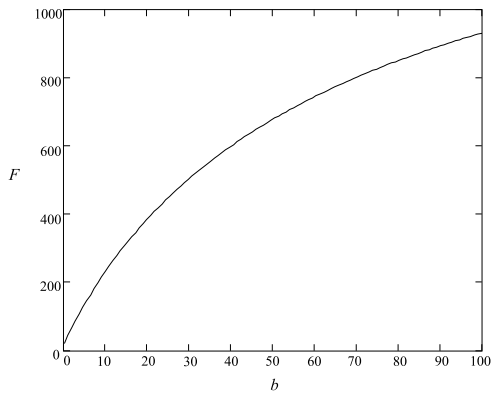


Fig. 4. The variation of the factor F with respect to the non-dimensional wall temperature b of 0.1–100.0.

from 0.1 to 100.0 with the other parameters at the baseline values. Outside the range of the fine grid region ($\eta > 6$), the potential flow streamline results are used. F increases with increasing b as shown in Fig. 4. Deposition systems often have a small value of b . Over the range of b from 0.1 to 2.0, F increases almost linearly with b . Since the thermophoretic force is proportional to the temperature gradient, the larger the temperature difference between the inlet and the wall, $T_\infty - T_w$, the larger the thermophoretic force. Note that the deposition flux (Eq. (18)) and efficiency (Eq. (20)) are directly proportional to the temperature difference between the inlet and wall temperatures and inversely proportional to F . This result is in agreement with Kusnadi and Greif's [7] finding using the similarity solution approach for stagnation deposition for a uniform inlet particle concentration boundary condition at an infinite distance from the wall.

4.3. Dependence on particle inlet location η_1

The quantity $F = x_w/x_i$ is calculated over a range of values of particle inlet elevations η_1 from 4 to 50 with the other parameters at the baseline values. The values of η_1 used are larger than the velocity boundary layer thickness $\eta_{\delta,velocity} = 2.4$. The results show that F increases almost linearly with η_1 (cf. Fig. 5). In Eq. (17), the value of F is proportional to $f(\eta_i = \eta_1)$; the integral and $f(\eta_{\delta,TH})$ are constants once the flow field parameters are fixed. The function $f(\eta_1)$ is nearly linear with η_1 , note that $f'(\eta) \rightarrow 1$ when $\eta \gg \eta_{\delta,velocity}$ so that F increases almost linearly with η_1 . Note that the deposition flux (Eq. (18)) and efficiency (Eq. (20)) are inversely proportional to F and therefore are also inversely proportional to the distance between the inlet elevation and the wall, η_1 .

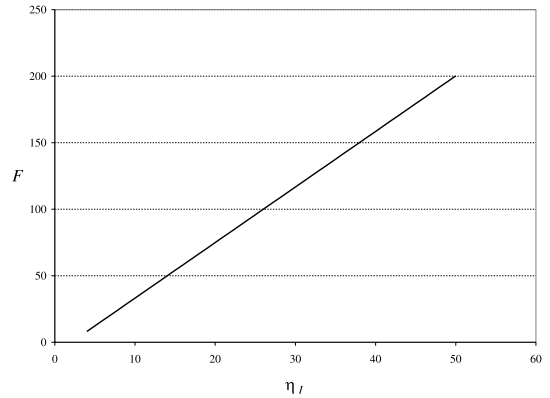


Fig. 5. The variation of the factor F with respect to the inlet elevation η_1 .

5. Dependence on Prandtl number, Pr

The factor $F = x_w/x_i$ is calculated over a range of values of the Prandtl number, Pr , from 0.2 to 10.0 with the other parameters at the baseline values. A minimum value of F is shown in Fig. 6 at $Pr \cong 5$.

For small values of Pr (large thermal boundary layer), F decreases (and the deposition flux increases) as Pr increases (and the thermal boundary layer decreases). The smaller the thermal boundary layer the larger the temperature gradient and thermophoretic force. Consequently, the particle paths will bend toward the wall and shorten the x component of particle travel before deposition. The factor F decreases (and the deposition flux increases) since the same number of particles then deposit over a shorter length under these conditions.

As $Pr \rightarrow \infty$, the thermal boundary layer becomes infinitesimal and particles deposit on the solid wall upon

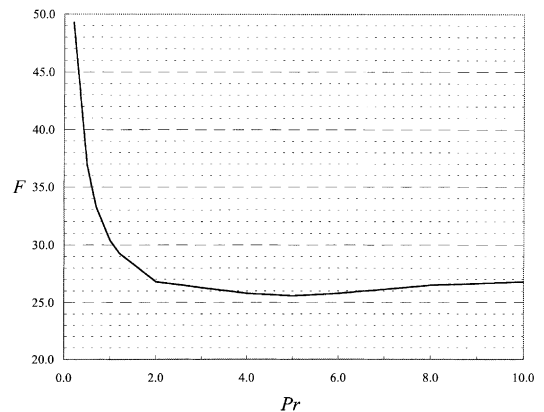


Fig. 6. The variation of the factor F with respect to the Prandtl number Pr . For the conditions of $\eta_1 = 10$, $b = 0.5$, and $K = 0.55$, a minimum value of F occurs at $Pr = 5$.

reaching the infinitesimally thick thermal boundary layer. For this condition, the distance the particles travel from the inlet to the thermal boundary layer becomes the controlling factor. The relationship between the x location where the particle enters the thermal boundary, $x_{\delta_{\text{TH}}}$, and the inlet x location, x_1 , is given by Eq. (16):

$$x_{\delta_{\text{TH}}} = x_1 \frac{f(\eta_1)}{f(\eta_{\delta_{\text{TH}}})}. \quad (27)$$

For a given inlet location (x_1, η_1) , the location at which the particle enters the thermal boundary, $x_{\delta_{\text{TH}}}$, is solely a function of $f(\eta_{\delta_{\text{TH}}})$. As $Pr \rightarrow \infty$, the thermal boundary layer thickness $\eta_{\delta_{\text{TH}}}$ approaches 0 and $f(\eta_{\delta_{\text{TH}}})$ approaches 0 and the particles will follow the gas streamlines outside the thermal boundary layer. For an infinitesimal thermal boundary layer, there will be no deposition on the wall. Thus, F approaches infinity (deposition flux approaches zero) as Pr approaches infinity.

With F decreasing as Pr increases for small Pr , and F increasing as Pr increases for large Pr , a minimum value of F exists for moderate Pr ; cf. Fig. 6. The Prandtl number corresponding to the minimum value of F must be determined from Eq. (17) for the specified conditions.

6. Conclusions

A methodology and solution for stagnation deposition with thermophoretic transport is presented for a generalized inlet particle boundary condition. The classical similarity solution requires a uniform inlet particle boundary condition at infinity; that is, the similarity solution is not valid (1) for either a non-uniform particle concentration at infinity, or (2) for an uniform particle concentration at a finite location $y_1 = C$, where y_1 is finite. In the present particle path approach, the uniform particle boundary condition at infinity is removed. For this approach, the particle distribution can be spatially variable and known at a finite distance y_1 from the wall. The problem of a hot wall with a corresponding ther-

mophoretic force away from the wall was also included using the particle path methodology developed in this work.

References

- [1] T. Li, Optical fiber communications, Fiber Fabrication, vol. 1, Academic, London, 1985.
- [2] S.A. Gokoglu, D.E. Rosner, Correlation of thermophoretically-modified small particle diffusional deposition rates in forced convection systems with variable properties, transpiration cooling and/or viscous dissipation, Int. J. Heat Mass Transfer 27 (1984) 639–646.
- [3] S.A. Gokoglu, D.E. Rosner, Thermophoretically augmented mass transfer rates to solid walls across laminar boundary layers, Am. Inst. Aeronaut. Astronaut. J. 24 (1986) 172–178.
- [4] F. Stratmann, H. Fissan, A. Papperger, S. Friedlander, Suppression of particle deposition to surfaces by the thermophoretic force, Aerosol Sci. Technol. 9 (1988) 115–121.
- [5] V.K. Garg, S. Jayaraj, Thermophoretic deposition in crossflow over a cylinder, J. Thermophys. 4 (1990) 115–116.
- [6] V.K. Garg, S. Jayaraj, Thermophoretic deposition over a cylinder, Int. J. Eng. Fluid Mech. 3 (1990) 175–196.
- [7] F. Kusnadi, R. Greif, Thermophoretic, convective and electrophoretic transport for stagnation flow on an infinite wall, J. Mater. Process. Manuf. Sci. 6 (1997) 147–160.
- [8] L. Waldmann, On the motion of spherical particles in nonhomogeneous gases, in: L. Talbot (Ed.), Rarefied Gas Dynamics, Academic Press, New York, 1961, pp. 323–344.
- [9] G.M. Graham, M.K. Alam, Outside vapor deposition (OVD) process with a wall jet burner, J. Chem. Vapor Deposition 6 (1997) 139–163.
- [10] S. Goldstein, Modern Developments in Fluid Dynamics II, 1950, pp. 631–632.
- [11] F.M. White, Fluid Mechanics, second ed., McGraw-Hill, New York, 1986.
- [12] H. Schlichting, Boundary Layer Theory, seventh ed., McGraw-Hill, New York, 1979.
- [13] L. Talbot, R.K. Cheng, R.W. Schefer, D.R. Willis, Thermophoresis of particles in a heated boundary layer, J. Fluid Mech. 101 (4) (1980) 737–758.